



OPEN Plasma metabolomic profiling of diabetic macular edema

Zi-yang Wang¹, Fang-yuan Yang^{1,2}, Si-Wei Cai³, Wei Tian⁴, Rong-rong Xie^{1,2}, Ran Sun¹ & Xiao-Rong Zhu^{1,2}✉

Diabetic macular edema (DME), a sight-threatening retinopathy, is a leading cause of vision loss in persons with diabetes mellitus. Despite strict control of systemic risk factors, a fraction of patients with diabetes developed DME, suggesting the existence of other potential pathogenic factors underlying DME. This study aimed to investigate the plasma metabolotype of patients with DME and to identify novel metabolite markers for DME. Biomarkers identified from this study will provide scientific insight and new strategies for the early diagnosis and intervention of DME. To match clinical parameters between case and control subjects, patients with DME (DME, $n=30$) or those with diabetes but without DME (Control, $n=30$) were assigned to the present case-control study. Distinct metabolite profiles of serum were examined using liquid chromatography-mass spectrometry (LC-MS). A total of 190 distinct metabolites between DME and Control groups were identified ($VIP>1$, Fold Change >1.5 or <0.667 , and $P<0.05$). The distinct metabolites between DME and Control groups were enriched in 4 KEGG pathways, namely, Glutamate Metabolism, Carnitine Synthesis, Oxidation of Branched Chain Fatty Acids, and Phytanic Acid Peroxisomal Oxidation. Finally, 4 metabolites were selected as candidate biomarkers for DME, namely, 5-Phospho-beta-D-ribosylamine, Succinic acid, Ascorbyl glucoside, and Glutathione disulfide. The area under the curve for these biomarkers were 0.693, 0.772, 0.762, and 0.771, respectively. This study suggested that impairment in the metabolism and 4 potential metabolites were identified as metabolic dysregulation associated with DME, which might provide insights into potential new pathogenic pathways for DME. 5-Phospho-beta-D-ribosylamine was first identified as a novel metabolite marker, with no previous reports linking it to diabetes or DME. This discovery may offer valuable insights into potential new pathogenic pathways associated with DME.

Keywords Type 2 diabetes, Diabetic macular edema, Metabolomics, Metabolic profiling, LC-MS

Abbreviations

DR	Diabetic retinopathy
NPDR	Non-proliferative diabetic retinopathy
DME	Diabetic macular edema
AMD	Age-related macular degeneration
PA	Phytanic acid
CSME	Clinical significant macular edema
DCCT	Diabetes Control and Complications Trial
WESDR	Wisconsin Epidemiology Study of Diabetic Retinopathy
OCT	Optical coherence tomography scanning
VEGF	Vascular endothelial growth factor
LC-MS	Liquid chromatography-mass spectrometry
T2D	Type 2 diabetes
HbA1c	Glycated hemoglobin A1c
BMI	Body mass index
SBP	Systolic blood pressure
DBP	Diastolic blood pressure
HDL	High density lipoprotein
LDL	Low density lipoprotein

¹Beijing Key Laboratory of Diabetes Research and Care, Department of Endocrinology, Beijing Tongren Hospital, Capital Medical University, Beijing 100730, China. ²Beijing Diabetes Institute, Beijing 100730, China.

³Department of Ophthalmology, Beijing Tongren Hospital, Capital Medical University, Beijing 100730, China.

⁴Outpatient Department, Beijing Tongren Hospital, Capital Medical University, Beijing 100730, China. ✉email: zhuxr_06@sina.com

TG	Triglyceride
PCA	Principal component analysis
PLS-DA	Projections to latent structures-discriminant analysis
AUC	Area under the curve
VIP	Variable important in the projection
QC	Quality control
UPLC	Ultra-performance liquid chromatography
Q-TOF MS	Quadrupole time-of-flight tandem mass spectrometry

Diabetic macular edema (DME) is a leading cause of vision loss in patients with diabetic retinopathy, particularly in those with non-proliferative diabetic retinopathy (NPDR) associated with type 2 diabetes. As the global prevalence of type 2 diabetes increases, the prevalence of DME is also anticipated to grow¹. It is projected that by 2030, the number of patients with clinical significant macular edema (CSME) will increase by 24.8% and reach 23.5 million. By 2045, these figures are expected to rise by 51.9%, reaching 28.61 million². Research indicates that over two-thirds of patients with DME have a visual acuity of less than 0.5, severely impacting their visual health³. Furthermore, the presence of DME consumes additional healthcare resources, leading to increased economic burdens and deteriorating quality of life⁴.

Understanding the underlying mechanisms of DME occurrence and pathogenesis, and identifying new drug targets, are crucial for preventing and advancing therapeutic strategies. Some studies suggest that clinical risk factors cannot account for all cases of severe diabetic retinopathy. It is estimated that these risk factors accounted for only 11% and 10% of the variability in DR risk in the Diabetes Control and Complications Trial (DCCT) and Wisconsin Epidemiology Study of Diabetic Retinopathy (WESDR) studies, respectively. The role of metabolic dysfunction in the development of DME is not yet fully understood either. A recent study suggested that elevated HbA1C and blood pressure confer a higher risk of DME development, whereas obesity and dyslipidemia do not⁵. The diagnosis of DME primarily relies on imaging tools such as fundus photography, optical coherence tomography (OCT) scanning, and fluorescein angiography. These methods are limited to detecting visible retinal damage and are unable to identify early lesions. The identification of biomarkers may aid in the early diagnosis of DME, facilitating early intervention and prevention for at-risk patients, thereby slowing disease progression⁶. Currently, the major treatments for DME include laser surgeries and anti-vascular endothelial growth factor (VEGF) therapies, with anti-inflammatory corticosteroids also playing an adjuvant role in DME management. As the first-line treatment for DME, although most patients respond well to anti-VEGF therapy, some exhibit poor responses, and long-term injections may lead to drug resistance⁷. This underscores the need to explore novel mechanisms of pathogenesis and therapeutic targets, as well as to identify early diagnostic biomarkers that could facilitate effective early diagnosis and intervention.

Biomarkers, as measurable indicators reflecting biological states, disease progression, and treatment responses, can significantly enhance the understanding of DME's pathogenesis. Metabolomics can detect the comprehensive and dynamic changes in endogenous metabolites within biological systems, including nucleic acids, proteins, lipids, and other small molecules. It is increasingly recognized as a powerful tool that complements genomic, transcriptomic, and proteomic data, which has been conducted in many diseases analysis for decades^{8,9}. However, there is limited research on the metabolomics of DME. Rhee et al. revealed the roles of amino acid metabolism and lipid metabolism in the progression of DME through an omics analysis of plasma samples from DME patients¹⁰. Our study builds upon this foundation, involving NPDR and DME patients aged between 40 and 60 years, aiming to refine the diagnosis, further identify meaningful biomarkers, and uncover the potential mechanisms of DME occurrence and early therapeutic targets.

Research design and methods

Patients

A case-control study was conducted. Clinical data and serum samples were collected from 60 type 2 diabetic patients with NPDR at TongRen Hospital. Of these, 30 patients diagnosed with DME were assigned to the DME group, while the remaining 30 patients with NPDR but without DME were included in the control group. Patients with glycated hemoglobin A1c (HbA1c) levels $\geq 7.0\%$ (53 mmol/mol) were selected for ocular phenotype screening. Exclusion criteria: (1) Individuals with other ocular diseases; (2) Acute or chronic liver disease, defined by serum levels of transaminases or alkaline phosphatase more than three times the upper limit of normal at screening; (3) Impaired renal function, defined as eGFR $< 30\text{ mL/min/1.73 m}^2$ (CKD-EPI); (4) Myocardial infarction, severe valvular heart disease, or symptomatic heart failure within the past 6 months, or left ventricular ejection fraction (by any method) < 45 . The sex and age of patients in the control group are matched with those in the DME group (Fig. 1).

Ethics statement

The study was conducted with the approval from the Ethics Committee of Beijing Tongren Hospital, Capital Medical University (TREC2023-KY059), and adhered to the Declaration of Helsinki. Written informed consent was obtained from each participant.

Baseline test

The medical histories of all participants were obtained, and each patient underwent a physical examination that included age, sex, disease duration, blood pressure, and body mass index (BMI) measurements. Patients also underwent blood and urine laboratory tests, including triglycerides (TG), high-density lipoprotein (HDL), low-density lipoprotein (LDL), serum creatinine (CREA), and HbA1c levels. All participants were informed that fasting blood samples would be collected in the morning between 7 a.m. and 9 a.m. following a 12-hour

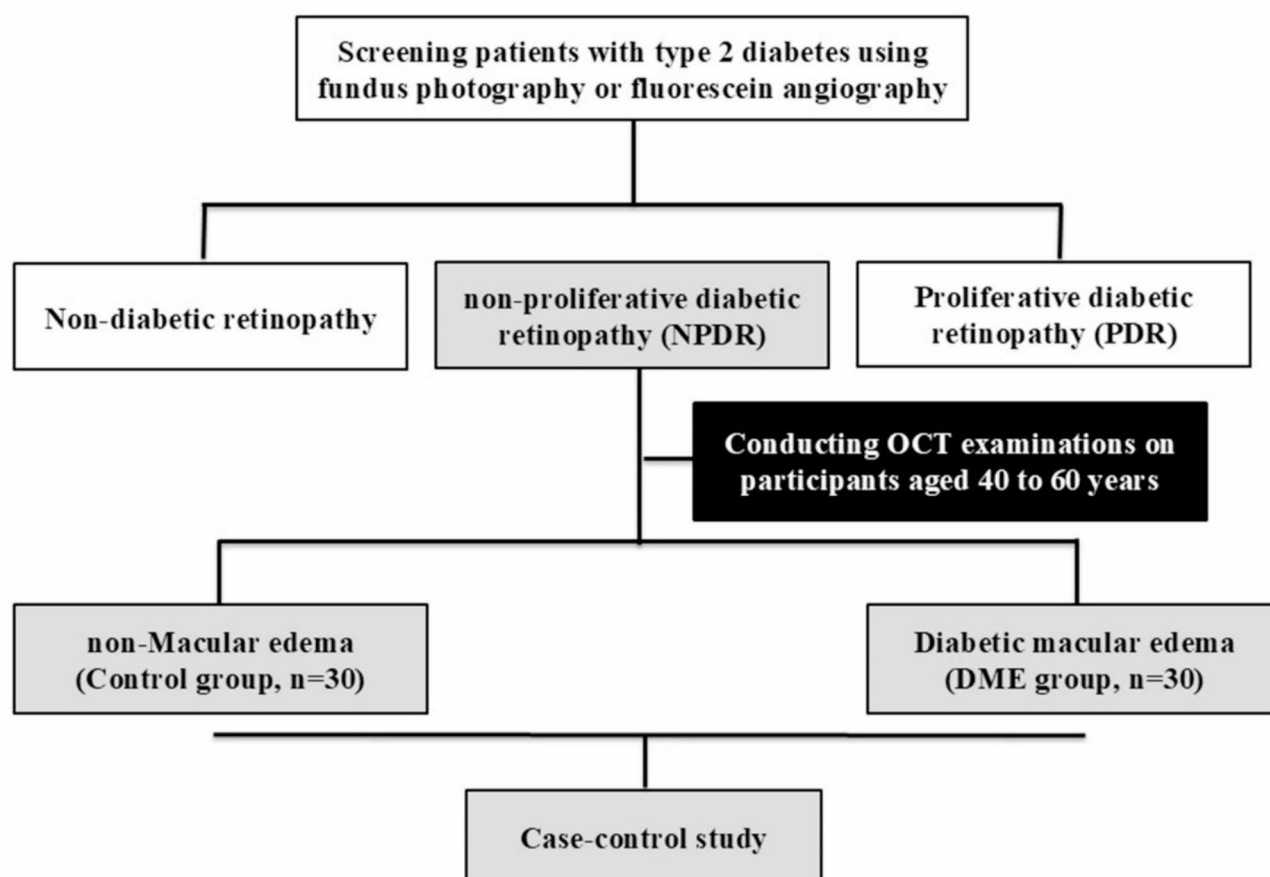


Fig. 1. Inclusion and exclusion flowchart of the case-control study. OCT, optical coherence tomography.

fast. Blood samples were collected using K2EDTA tubes, which were centrifuged at 3000 g for 10 min at 4 °C to separate plasma from whole blood. Plasma aliquots were stored at − 80 °C.

Eye examination

The patients underwent routine ophthalmological examinations. All patients underwent OCT examinations and, simultaneously, either fundus photography or fundus fluorescein angiography for diabetic retinopathy. In accordance with the Early Treatment Diabetic Retinopathy Study (ETDRS) and the International Clinical Diabetic Retinopathy Disease Severity Scale, patients were diagnosed and graded by at least two retinal specialists. Fundus photography (TRCNW7SF; Topcon Co. Tokyo, Japan) and OCT (HD-OCT; Carl Zeiss Meditech, Dublin, CA, USA) were performed during the initial diagnosis. Patients who represented any apparent retinal thickening (central macular thickness (CMT) ≥ 275 μm with OCT) or hard exudates in posterior pole, meeting the following criteria with FFA as well, would be diagnosed with DME: (1) Retinal thickening at or within 500 μm of the center of the macula; (2) Hard exudates at or within 500 μm of the center of the macula, with associated retinal thickening; (3) Zones of retinal thickening of one disc diameter or larger, with any part located within one disc diameter of the macula center^{11–13}. Meeting the criteria based on FFA is necessary to be enrolled in DME group. In cases of discordance between evaluators, the ophthalmologists reviewed the images and reached a consensus on the final interpretation. (Fig. 2).

Sample preparation

Before analysis, frozen plasma samples were thawed and dissolved at 4 °C. Acetonitrile/methanol (75:25 v/v, 300 μL) was added to the serum (100 μL) in a 1.5-mL tube to precipitate proteins. After vortexing for 60 s, the mixture was allowed to stand for 10 min and then centrifuged at 12,000 rpm for 10 min at 4 °C. The supernatant was transferred to a new Eppendorf tube and evaporated to dryness using a speed-vac concentrator. The resulting residues were re-suspended in 100 μL of mobile phase prior to LC-MS analysis. Quality control (QC) samples were prepared by mixing equal amounts of serum from each sample and following the same procedures as for the test samples to extract metabolites. One QC sample was inserted every five test samples before and after operation.

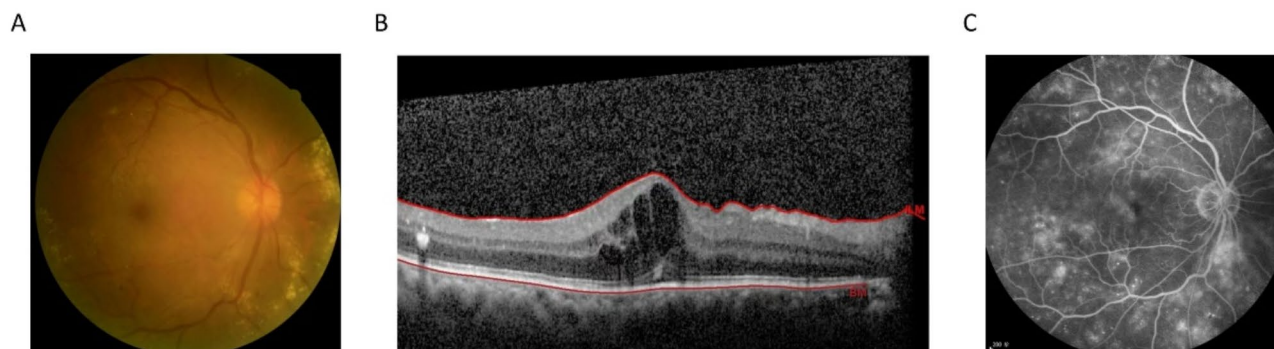


Fig. 2. Fundus imaging signs of a patient with diabetic macular edema (DME) were shown. (a) Image captured by fundus photography. (b) Images captured by optical coherence tomography (OCT). (c) Image captured by fluorescein fundus angiography (FFA). Parts a, b, and c were derived from the same eye.

LC-MS (liquid chromatography-mass spectrometry) analysis

The ultra-performance liquid chromatography (UPLC) coupled with quadrupole time-of-flight tandem mass spectrometry (Q-TOF MS) was conducted using the Nexera X2 system (Shimadzu, Japan) in combination with a Triple TOF 5600+ mass spectrometer (AB SCIEX, USA), as previously described¹⁴. Briefly, chromatographic separation was achieved using a ZORBAX Eclipse Plus C18 column (2.1 × 100 mm, 3.5 μm, Agilent, USA) maintained at 45 °C. The sample injection volume was 10 μL in full loop mode, and the mobile phase flow rate was set at 0.5 mL/min. In reverse-phase liquid chromatography (RPLC) mode, gradient elution was performed using the following solvent system: (A) 0.1% formic acid in water, and (B) acetonitrile with 0.1% formic acid. The gradient started at 98% A, reduced to 10% A over 13 min, held at 10% A for 3 min, and then returned to 98% A, held for 4 min. Mass spectrometry analysis was conducted using a Triple TOF 5600+ mass spectrometer equipped with an electrospray ionization (ESI) source. Data acquisition was performed in both positive and negative ionization modes for each chromatographic separation. The capillary voltages were set to 2500 V and 3000 V, with cone gas flow at 50 L/h, desolvation gas flow at 600 L/h, source temperature at 120 °C, and desolvation temperature at 500 °C. The scan range was set from 50 to 1500 m/z in full-scan mode, and data were collected in centroid mode. Independent reference lock-mass ions were used to ensure mass accuracy during data acquisition via Analyst TF 1.6 and MarkerView 1.2.1.

Metabolites identification

Raw UPLC Q-TOF MS data were pre-processed using MarkerView software for retention time alignment, peak discrimination, filtering, alignment, matching, and metabolite identification, generating a peak table with retention time (RT), m/z values, and corresponding peak intensities. Multivariate analyses, including unsupervised principal component analysis (PCA) and supervised projections to latent structures-discriminant analysis (PLS-DA), were performed using the MetaboAnalyst 4.0 platform (<http://www.metaboanalyst.ca/>) to identify metabolite differences between the two groups. The identified metabolite ions were matched based on m/z and cross-referenced with the Human Metabolome Database (HMDB, <http://www.hmdb.ca/>)¹⁵. The mass tolerance for HMDB searches was set at 0.05 Da. Chromatographic retention behavior was considered to minimize false-positive matches. An overview of workflow with respect to the comprehensive analysis of metabolomics in type 2 diabetes patients with DR is summarized in Fig. 3.

Statistical analysis

The Mann-Whitney U test was first employed to compare the DME and control groups. Multivariate analyses, including PCA and PLS-DA, were conducted using MetaboAnalyst 4.0 to investigate group distribution and metabolic differences. Cross-validation of PLS-DA models was carried out using a 10-fold method with unit variance scaling. The R^2 parameter was used to evaluate model fit, while Q^2 assessed predictive power; negative or very low Q^2 values indicated non-significant differences between groups. The PLS-DA model was designed to remove variation in the X matrix not correlated with the Y matrix, usually requiring only one predictive component for class discrimination.

Comparisons of integrated region intensities between the two groups were performed using Welch's t-test (two-tailed) via MetaboAnalyst 4.0, with p-values < 0.05 considered statistically significant. Volcano plots were generated based on a combination of fold-change and t-test results, identifying peaks with statistically significant differences. These peaks were subsequently used for multivariate pattern recognition. Peaks exhibiting consistent up- or down-regulation were then subjected to box-plot analysis, hierarchical clustering, and metabolic pathway analysis.

Pathway analysis

In this study, differential chemical metabolites were evaluated utilizing the MetaboAnalyst web portal for pathway analysis and visualization (<http://www.metaboanalyst.ca/>). Additionally, pathway enrichment statistics were further investigated using Metabolite Set Enrichment Analysis (MSEA) (<http://www.msea.ca/MSEA/face>).

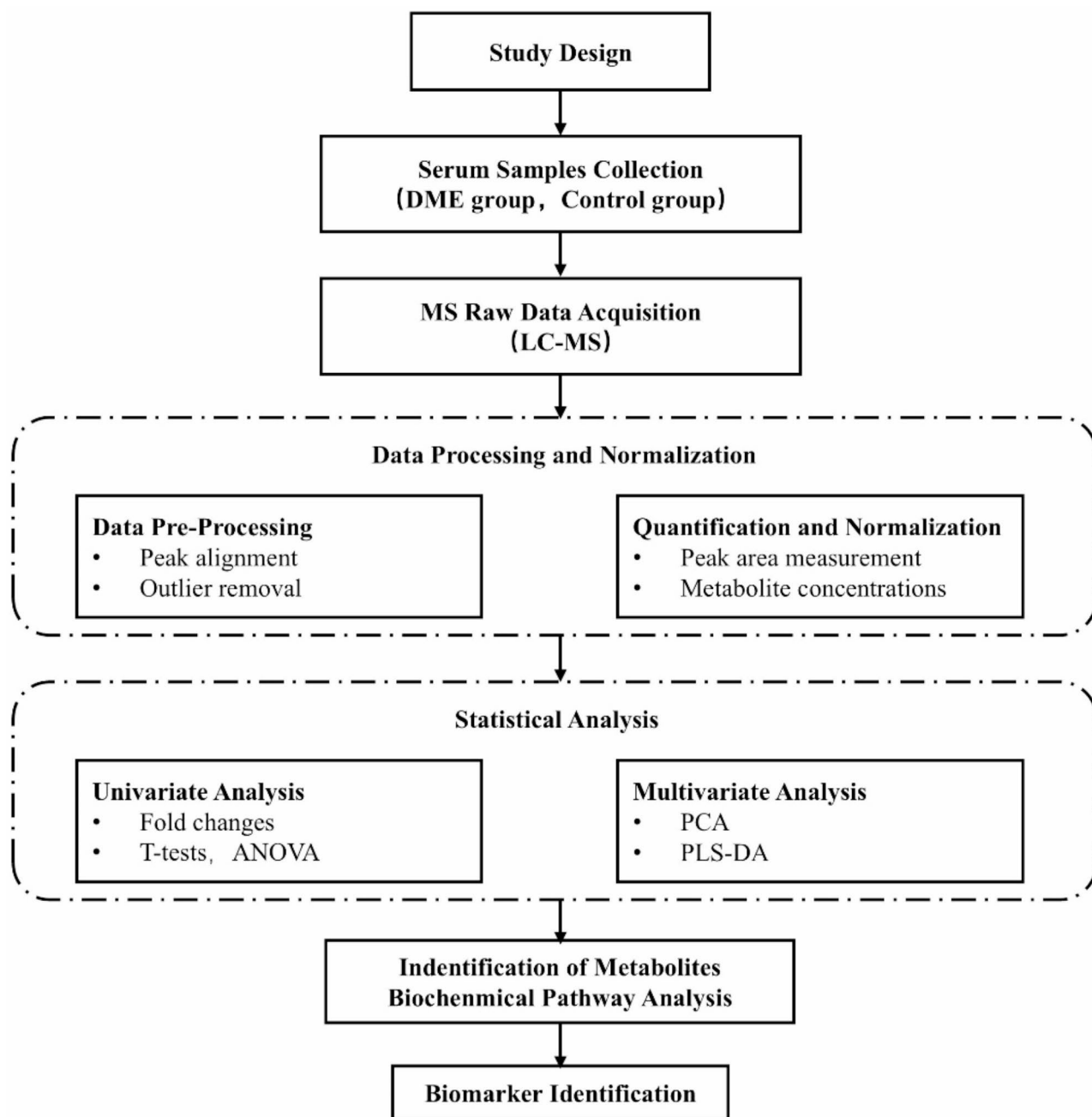


Fig. 3. Workflow overview of the comprehensive analysis of metabolomics in type-2 diabetes patients with DR.

[s/Home.jsp](#)). Pearson's correlation coefficient (r) was calculated to assess the relationships among biomarkers ($P < 0.05$).

Screening for candidate plasma biomarkers of DME

Metabolites involved in the four pathways mentioned above were further selected from the 190 identified metabolites. Furthermore, ROC analysis was performed on the data by utilizing pROC [1.18.0] within R studio software [4.2.1], and the resultant data was visualized using ggplot2 [3.4.4]. Additionally, the data was visualized through ggplot2 [3.4.4] in R studio software [4.2.1], and the adopted statistical method was the Wilcoxon rank sum test, where $**P < 0.01$ and $***P < 0.001$. The substances with an AUC value greater than 0.6 and $P < 0.01$ will be selected as the candidate plasma biomarkers of DME.

Results

Demographic and clinical information

Based on the exclusion criteria for the case-control study, 30 patients with DME were designated as case subjects, while 30 patients with type 2 diabetes and NPDR were assigned as control subjects (Fig. 1). Table 1 summarizes the characteristics of the study participants. No significant differences were observed between the two groups in terms of age, sex, duration of diabetes, BMI, blood pressure, creatinine, triglycerides, LDL, HDL, glycated hemoglobin, or urea nitrogen levels. However, a notable difference in urinary albumin excretion rate (UAER) was identified between the DME group and the control group, which we hypothesize may be related to the occurrence of diabetic nephropathy.

Models analysis

To enhance the separation between the two groups, partial least squares discriminant analysis (PLS-DA) was employed to visualize metabolic differences. All models underwent 7-fold cross-validation and 200 permutation tests. The validity of the models with respect to overfitting was evaluated using the R^2 parameter, while the predictive ability was quantified by Q^2 . In the PLS-DA model, the R^2 and Q^2 values were 0.82 and 0.42, respectively. These results indicate that the PLS-DA model demonstrated strong applicability and was effective in distinguishing case groups from control groups (Fig. 4).

Pathway analysis

A total of 190 metabolites were identified as significantly altered between the DME and control subject groups. These metabolites were enriched in 27 pathways from the KEGG PATHWAY database^{16–18}, with four pathways showing significant enrichment ($P < 0.05$). These pathways included glutamate metabolism, carnitine biosynthesis, branched-chain fatty acid oxidation, and phytanic acid peroxisomal oxidation. The enrichment ratio for the top pathways and the network relationships among all enriched pathways are presented in Fig. 5.

Biomarkers for DME diagnosis

Four metabolites, which were involved in the four pathways mentioned above and had an AUC value greater than 0.6 and $P < 0.01$, were selected from the 190 identified metabolites as the candidate plasma biomarkers of DME.

	Control	DME	P-value
n	30	30	–
Gender (male/female)	22/8	22/8	–
Diabetic retinopathy	NPDR	NPDR	–
Age (years)	52.7 (41–60)	54 (36–60)	0.289
Diabetes duration (years)	11.90 ± 5.11	12.14 ± 6.67	0.877
BMI (kg/m ²)	25.39 ± 2.34	25.37 ± 3.40	0.983
SBP (mmHg)	130.5 (95–165)	132.7 (103–192)	0.859
DBP (mmHg)	78.67 ± 11.55	78.33 ± 11.28	0.910
CREA (μmol/L)	65.9 (33.6–117.8)	180 (40.3–180)	0.067
TG (mmol/L)	1.85 (0.47–12.54)	1.76 (0.52–8.47)	1.000
LDL (mmol/L)	2.71 ± 0.78	2.50 ± 0.74	0.308
HDL (mmol/L)	1.08 (0.54–1.90)	1.03 (0.62–1.60)	0.762
HbA1c (%)	8.98 (6.90–12.20)	8.34 (5.70–11.60)	0.085
BUN (mmol/L)	5.89 ± 1.60	6.00 ± 1.79	0.803
UAER (μg/min)	8.39 (4.69–75.5)	58.54 (9.45–715.96)	0.029*
Diabetic nephropathy	11	15	0.435
Insulin injection	10	12	0.789
Insulin secretagogues	4	2	–
α-Glucosidase inhibitors	7	9	–
Metformin	15	11	–
SGLT2i	2	4	–
DPP-4	3	5	–
GLP-1RA	1	2	–

Table 1. Baseline demographics in this study. * $P < 0.05$. Data correspond to normal distribution, including diabetes duration, BMI, DBP, LDL and BUN, were performed with T test and presented in mean ± sd. Non-normally distributed data, such as age, SBP, CREA, TG, HDL, HbA1c and UAER were performed with Mann-Whitney U test and presented in median (25th,75thinterval). NPDR non-proliferative diabetic retinopathy, SBP systolic blood pressure, DBP diastolic blood pressure, CREA creatinine, TG triglyceride, UAER urinary albumin excretion rates. HDL high-density lipoprotein, LDL low-density lipoprotein, SGLT2i Sodium-glucose linked transporter 2 inhibitor, DPP-4 dipeptidyl peptidase-4 inhibitors, GLP-1RA Glucagon-like peptide-1 receptor agonists.

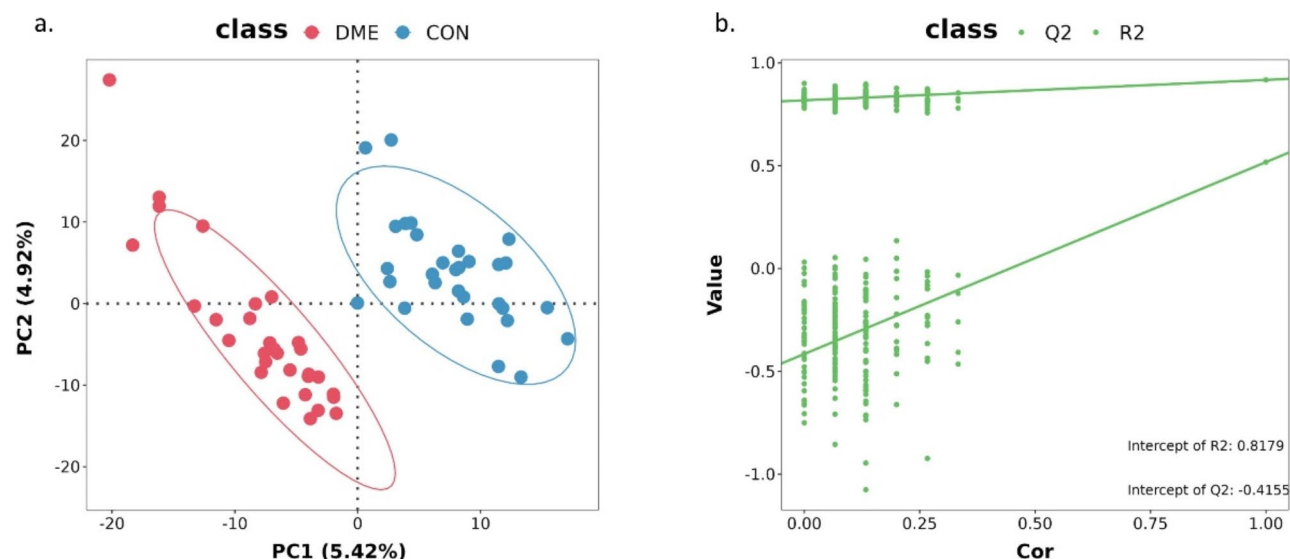


Fig. 4. Score plots of the PCA and PLS-DA models. **(a)** Score plot of the PCA model for samples collected from 2 isolates of sample data; **(b)** the 2 groups were well separated in the PLS-DA score plot, indicating that they had markedly different metabolic characteristics.

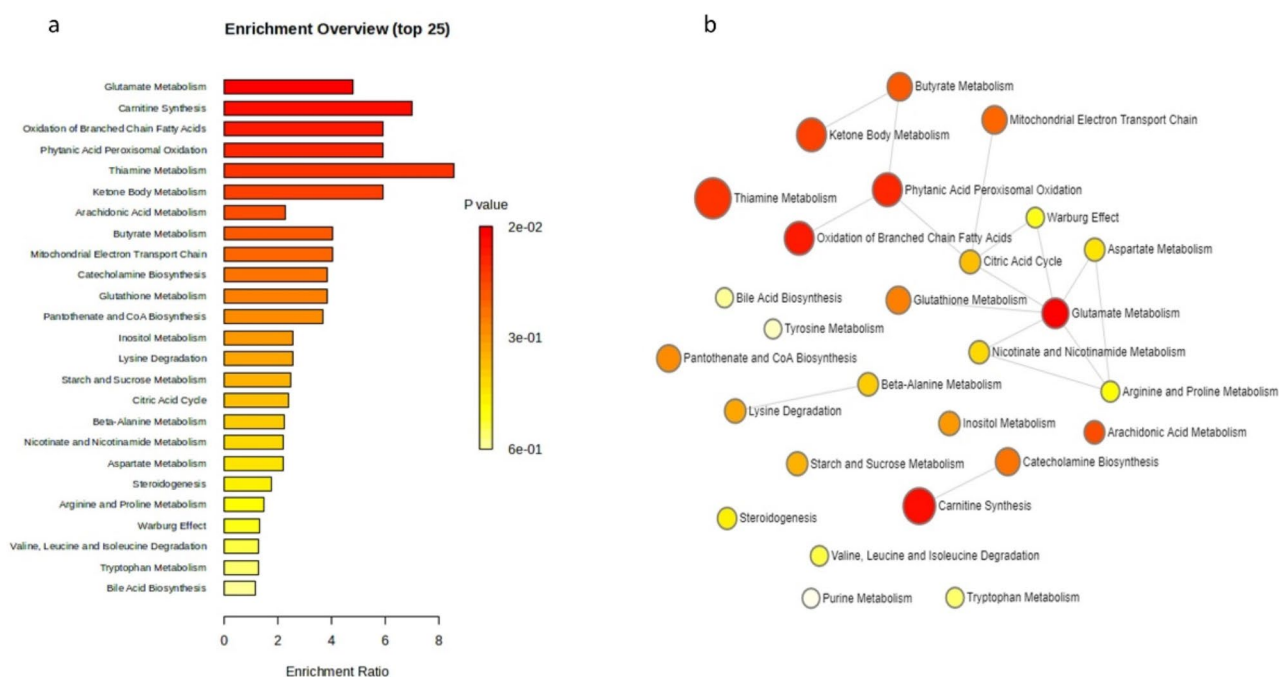


Fig. 5. Metabolomics pathway analysis. **(a)** Pathway enrichment analysis overview, in which four pathways were enriched, including Glutamate Metabolism, Carnitine Synthesis, Oxidation of Branched Chain Fatty Acids and Phytanic Acid Peroxisomal Oxidation. ($P < 0.05$). **(b)** Network of the enriched pathways. Each node represents a metabolite set with its color based on its p value, and its size is based on fold enrichment (hits/expected). Two metabolites sets are connected by an edge if the number of their shared metabolites is over 25% of the total number of their combined metabolite sets.

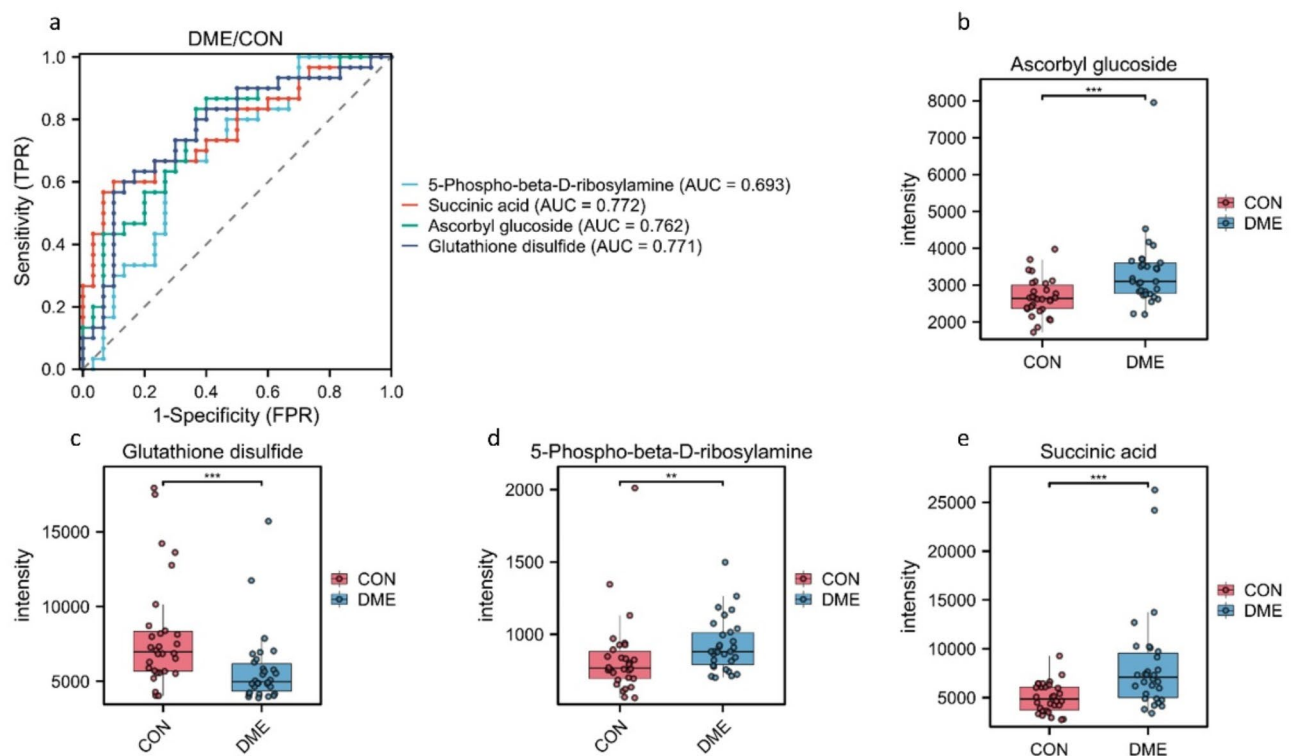


Fig. 6. Receiver operating characteristic (ROC) curve analysis was performed to evaluate the use of metabolites as biomarkers for DME. (a) The AUC of 4 biomarkers (5-Phospho-beta-D-ribosylamine, Ascorbyl glucoside, Succinic acid, Glutathione disulfide) are 0.693, 0.772, 0.762, 0.771, respectively. (b–e) The intensity level of 4 biomarkers in DME and control group, respectively (Median \pm IQR). ** p < 0.01, *** p < 0.001.

These are 5-Phospho-beta-D-ribosylamine, Succinic acid, Ascorbyl glucoside and Glutathione disulfide. The AUCs of these biomarkers were 0.693 (P < 0.01), 0.772 (P < 0.001), 0.762 (P < 0.001), 0.771 (P < 0.001), respectively (Fig. 6).

Discussion

DME is a common ocular complication of diabetes and has now become one of the leading causes of blindness in diabetic patients. This condition arises from an imbalance of fluid between the retinal vasculature and the extracellular space, often secondary to the disruption of the blood-retinal barrier and increased microvascular permeability. In an epidemiological analysis of DR, Hou et al. reported that among 50,564 diabetic patients aged 18 to 74, the incidence of DME accounted for approximately 23% of cases of vision-threatening diabetic retinopathy (VTDR)¹⁹. Additionally, a survey of medical insurance data from 2009 to 2018 revealed a rising trend in the incidence of DME, with an increasing proportion of VTDR cases attributed to DME²⁰. These findings suggest that DME has increasingly become a significant threat to the vision of diabetic patients.

Recent advances have been made in understanding the pathogenesis of DME. Hyperglycemia can lead to disruptions in various metabolic pathways, including increased polyol production and oxidative stress, which induce the expression of VEGF, promote inflammatory responses, and exacerbate capillary leakage, thereby accelerating the progression of DME^{21,22}. Previous studies have confirmed a clear association between VEGF, secondary inflammation, and the pathogenesis of DME²³. Currently, the primary treatment modalities for DME include laser surgery and anti-VEGF therapy; however, these interventions are typically employed in the later stages of the disease. Moreover, frequent intravitreal injections can lead to ocular complications, are costly, and may not yield favorable outcomes or prognosis in some patients^{24,25}. This underscores the need to explore novel mechanisms of pathogenesis and therapeutic targets, as well as to identify early diagnostic biomarkers that could facilitate effective early diagnosis and intervention.

In this study, we employed LC-MS-based metabolomics analysis to identify differential metabolic pathways and metabolites in the plasma of diabetic patients with and without DME. Ultimately, the distinct metabolites were enriched in four metabolic pathways, and 4 metabolites were selected as candidate biomarkers for DME. In our study, three substances with an AUC value greater than 0.7 and one substance with an AUC value greater than 0.6 will be selected for discussion. Although the AUC results in this study are not outstanding compared with those of previous metabolomics studies, this is an exploratory study, which may offer valuable insights into potential new pathogenic pathways associated with DME. Studies on DME metabolomics remain limited. Rhee et al., using gas chromatography time-of-flight mass spectrometry (GC-TOF-MS), conducted metabolic profiling on plasma samples collected from diabetic patients with over 15 years of disease duration,

prioritizing those aged over 60. The study employed OCT for fundus evaluation and revealed abnormalities in several metabolic pathways, including amino acid and lipid metabolism. Specific alterations were observed in carbohydrate metabolism, phenylalanine metabolism, alanine metabolism, aspartate metabolism, glutamate metabolism, arginine metabolism, and oxidative lipid metabolism¹⁰. Our study involved a relatively larger sample size, including patients aged 40 to 60 years with DME associated with diabetic retinopathy. By integrating results from fundus photography, OCT, and fundus fluorescein angiography, we established a clear diagnosis of DME. This comprehensive approach allows us to effectively minimize the influence of randomness and other confounding variables on our findings, thereby ensuring the rigor of our research. Based on this, we have advanced and supplemented the understanding of the pathogenesis and biomarkers of DME. Notably, we were the first to report abnormal levels of 5-phospho- β -D-ribosylamine in DME patients, suggesting that nucleotide metabolism may play a critical role in the occurrence of DME. The metabolic dysfunction in the phytanic acid peroxisomal pathway highlights the importance of phytanic acid degradation in DME, identifying it as a potential future target for diagnosis and treatment. Furthermore, based on our findings, and integrating previous research on DR and age-related macular degeneration (AMD), we propose additional potential mechanisms involving metabolites such as succinic acid, glutathione, and carnitine in the development of diabetic macular edema.

In this study, we found that the plasma concentration of 5-phospho- β -D-ribosylamine in the DME group was significantly higher than that in the control group. Previous research has also reported elevated levels of purines and pyrimidines in the plasma of DR patients, along with disruptions in the metabolic pathways of these nucleotides. Additionally, increased uric acid levels have been observed in both the plasma and aqueous humor of DME patients^{10,26–28}. 5-Phospho- β -D-ribosylamine is a key precursor in the synthesis of purine nucleotides and an important intermediate in pyrimidine biosynthesis. The degradation of purines and pyrimidines leads to the production of uric acid. Elevated plasma uric acid can directly damage endothelial and vascular smooth muscle cells and inhibit nitric oxide (NO) synthesis through the renin-angiotensin system, ultimately resulting in microvascular injury. Dysregulation in purine and pyrimidine metabolism may disturb uric acid levels in plasma, contributing to microvascular damage and the progression of DME²⁹. As a precursor in purine and pyrimidine biosynthesis, we propose that the abnormal levels of 5-phospho- β -D-ribosylamine may influence uric acid concentrations through these pathways, thereby increasing the occurrence of DME.

In recent years, a growing body of research has highlighted the role of succinic acid in the regulation of inflammation. As a critical intermediate metabolite in several metabolic pathways, succinic acid is involved in the production and degradation of reactive oxygen species (ROS). In our study, we found that the plasma concentration of succinic acid in DME patients was significantly higher than that in the control group. Li et al. demonstrated that intracellularly, succinic acid promotes VEGF expression via activation of gene promoters dependent on HIF-1 α . Extracellularly, succinic acid activates the G-protein-coupled receptor 91 (GPR91) and induces VEGF expression, exacerbating DME³⁰.

An important mechanism in DME progression is the increased production of polyols. Under hyperglycemic conditions, the activity of the rate-limiting enzyme aldose reductase in this pathway increases, converting glucose into sorbitol³¹. This process consumes large amounts of NADPH, inhibiting the conversion of reduced glutathione (GSH) to oxidized glutathione (GSSH), thereby reducing the GSH/GSSH ratio³². In our study, we observed a significant decrease in plasma GSSH levels in DME patients compared to the control group. Based on previous research, it is known that the levels of glutamate and cysteine—precursors for GSH synthesis—are also markedly reduced in the plasma of DME patients¹⁰. Similar disruptions in the metabolic pathways of these two amino acids have been reported in DR patients³³. We hypothesize that these alterations contribute to an overall reduction in both GSH and GSSH levels. The decline in both the relative ratio and absolute levels of GSH further exacerbates oxidative stress, promoting inflammation and microvascular damage, thus increasing the occurrence of DME.

We identified several additional metabolic pathway abnormalities in DME patients. Previous studies have revealed significant associations between fatty acid oxidation and amino acid metabolism, particularly the glutamate metabolic pathway, with the onset and progression of DR and DME. Our findings support this view^{10,34}. Moreover, we discovered abnormalities in the carnitine metabolism and phytanic acid peroxisomal metabolism pathways in DME patients. Ancel et al. observed increased levels of methylglutaryl carnitine in the plasma of DR patients³⁵. Additionally, Kevin et al. identified abnormalities in acylcarnitine levels during metabolomic analyses of patients with AMD³⁶. These findings suggest that carnitine metabolism may be linked to various diabetic ocular complications and could serve as a potential target for future diagnostic and therapeutic interventions. Grochowski et al. observed a consistent elevation in glutamate levels in both the aqueous humor and serum of diabetic patients. It was also observed that acylcarnitine levels were elevated in the aqueous humor of DM patients. The above findings corroborate our previous observations, in which the DME patients' glutamate metabolism and carnitine synthesis shows in disorder³⁷. Phytanic acid (PA) is a methyl-branched fatty acid found in the human diet, which undergoes complete oxidation in the peroxisomes and mitochondria after ingestion. During multiple rounds of β -oxidation, ROS can be generated, leading to cellular damage³⁸. Röncke et al. found that PA induces significant changes in Ca²⁺ homeostasis in hippocampal neurons, astrocytes, and oligodendrocytes, triggering apoptosis³⁹, which may be related to retinal cell damage observed in DME patients.

Exploring the pathogenesis and biomarkers for the diagnosis and treatment of DME through metabolomics offers significant advantages. However, this field is still in early stages, with limited reports and inconsistent findings across studies. Our research, being exploratory in nature, has certain limitations, including a relatively small sample size, which is insufficient to make definitive conclusions about the metabolic state of DME patients. Larger sample sizes and cohort studies are needed to validate these findings. The exact mechanisms underlying this disease are complex and require further investigation.

Overall, we performed a metabolomic analysis comparing DME patients with control subjects and identified unique metabolic characteristics in the DME group. Four differential metabolic pathways were enriched and

four distinct metabolites potentially related to the pathogenesis of DME were identified from the above selected pathways. For the first time, we reported abnormal levels of 5-phospho- β -D-ribosylamine in DME patients, suggesting that nucleotide metabolism may play a critical role in pathogenesis of DME. Our findings supplement and refine the existing understanding of DME pathogenesis and propose potential targets for its diagnosis and treatment.

Data availability

The datasets used and analyzed during the current study are available from the corresponding author (X.R.Z) upon reasonable request.

Received: 6 November 2024; Accepted: 17 March 2025

Published online: 23 March 2025

References

- Li, Z. et al. Nomogram-based prediction of clinically significant macular edema in diabetes mellitus patients. *Acta Diabetol.* **59**, 1179–1188 (2022).
- Teo, Z. L. et al. Global prevalence of diabetic retinopathy and projection of burden through 2045: systematic review and meta-analysis. *Ophthalmology* **128**, 1580–1591 (2021).
- Ciulla, T. A., Pollack, J. S. & Williams, D. F. Visual acuity outcomes and anti-VEGF therapy intensity in diabetic macular oedema: a real-world analysis of 28 658 patient eyes. *Br. J. Ophthalmol.* **105**, 216–221 (2021).
- Li, Y. et al. Global research trends and future directions in diabetic macular edema research: A bibliometric and visualized analysis. *Med. (Baltim)*. **103**, e38596 (2024).
- Haliyur, R., Marwah, S., Mittal, S., Stein, J. D. & Shah, A. R. Demographic and metabolic risk factors associated with development of diabetic macular edema among persons with diabetes mellitus. *Ophthalmol. Sci.* **4**, 100557 (2024).
- Sharma, S. et al. Tear protein markers for diabetic retinopathy and diabetic macular edema—towards an early diagnosis and better prognosis. *Semin Ophthalmol.* **39**, 440–450 (2024).
- Apte, R. S., Chen, D. S. & Ferrara, N. VEGF in signaling and disease: beyond discovery and development. *Cell* **176**, 1248–1264 (2019).
- Holmes, E., Wilson, I. D. & Nicholson, J. K. Metabolic phenotyping in health and disease. *Cell* **134**, 714–717 (2008).
- Nicholson, J. K. & Lindon, J. C. Systems biology: Metabonomics. *Nature* **455**, 1054–1056 (2008).
- Rhee, S. Y. et al. Plasma amino acids and oxylipins as potential multi-biomarkers for predicting diabetic macular edema. *Sci. Rep.* **11**, 9727 (2021).
- Grading diabetic retinopathy. from stereoscopic color fundus photographs—an extension of the modified Airline House classification. ETDRS report number 10. Early Treatment Diabetic Retinopathy Study Research Group. *Ophthalmology* **98**, 786–806 (1991).
- Wilkinson, C. P. et al. Proposed international clinical diabetic retinopathy and diabetic macular edema disease severity scales. *Ophthalmology* **110**, 1677–1682 (2003).
- Fan, C., Wang, Y., Ji, Q., Zhao, B. & Xie, J. Comparison of clinical efficacy of intravitreal ranibizumab with and without triamcinolone acetate in macular edema secondary to central retinal vein occlusion. *Curr. Eye Res.* **39**, 938–943 (2014).
- Liu, J. et al. Metabolomics-based clinical efficacy and effect on the endogenous metabolites of Tangzhiqing tablet, a Chinese patent medicine for type 2 diabetes mellitus with hypertriglyceridemia. *Evid. Based Complement. Altern. Med.* **2018**, 5490491. (2018).
- Wishart, D. S. et al. HMDB: a knowledgebase for the human metabolome. *Nucleic Acids Res.* **37**, D603–610 (2009).
- Kanehisa, M., Furumichi, M., Sato, Y., Matsuura, Y. & Ishiguro-Watanabe, M. KEGG: biological systems database as a model of the real world. *Nucleic Acids Res.* **53**, D672–D677 (2025).
- Kanehisa, M. & Goto, S. KEGG: kyoto encyclopedia of genes and genomes. *Nucleic Acids Res.* **28**, 27–30 (2000).
- Kanehisa, M. Toward understanding the origin and evolution of cellular organisms. *Protein Sci.* **28**, 1947–1951 (2019).
- Hou, X. et al. Prevalence of diabetic retinopathy and vision-threatening diabetic retinopathy in adults with diabetes in China. *Nat. Commun.* **14**, 4296 (2023).
- Lundeen, E. A. et al. Trends in the prevalence and treatment of diabetic macular edema and vision-threatening diabetic retinopathy among commercially insured adults aged < 65 years. *Diabetes Care.* **46**, 687–696 (2023).
- Noma, H., Yasuda, K. & Shimura, M. Involvement of cytokines in the pathogenesis of diabetic macular edema. *Int. J. Mol. Sci.* **22**, (2021).
- Tan, G. S., Cheung, N., Simó, R., Cheung, G. C. & Wong, T. Y. Diabetic macular oedema. *Lancet Diabetes Endocrinol.* **5**, 143–155 (2017).
- Simó, R., Sundstrom, J. M. & Antonetti, D. A. Ocular anti-VEGF therapy for diabetic retinopathy: the role of VEGF in the pathogenesis of diabetic retinopathy. *Diabetes Care.* **37**, 893–899 (2014).
- Sorour, O. A. et al. Persistent diabetic macular edema: Definition, incidence, biomarkers, and treatment methods. *Surv. Ophthalmol.* **68**, 147–174 (2023).
- Simó, R. & Hernández, C. Novel approaches for treating diabetic retinopathy based on recent pathogenic evidence. *Prog Retin Eye Res.* **48**, 160–180 (2015).
- Xia, J., Wang, Z. & Zhang, F. Association between related purine metabolites and diabetic retinopathy in type 2 diabetic patients. *Int. J. Endocrinol.* **2014**, 651050 (2014).
- Xia, J. F. et al. Correlations of six related pyrimidine metabolites and diabetic retinopathy in Chinese type 2 diabetic patients. *Clin. Chim. Acta.* **412**, 940–945 (2011).
- Qin, Y. J. et al. Elevated level of uric acid, but not glucose, in aqueous humor as a risk factor for diabetic macular edema in patients with type 2 diabetes. *Retina* **42**, 1121–1129 (2022).
- Rivera-De-la-Parra, D. et al. Association between uric acid and referable diabetic retinopathy in patients with type 2 diabetes. *Sci. Rep.* **14**, 12968 (2024).
- Li, Y. et al. Succinate induces synovial angiogenesis in rheumatoid arthritis through metabolic remodeling and HIF-1 α /VEGF axis. *Free Radic Biol. Med.* **126**, 1–14 (2018).
- Romero-Aroca, P. et al. Diabetic macular edema pathophysiology: vasogenic versus inflammatory. *J. Diabetes Res.* **2016**, 2156273. (2016).
- Singh, M., Kapoor, A. & Bhatnagar, A. Physiological and pathological roles of aldose reductase. *Metabolites* **11**, (2021).
- Wang, H. et al. Plasma and vitreous metabolomics profiling of proliferative diabetic retinopathy. *Invest. Ophthalmol. Vis. Sci.* **63**, 17 (2022).
- Diniz, T. G. et al. Metabolomic analysis of retinopathy stages and amputation in type 2 diabetes. *Clin. Nutr. ESPEN.* **61**, 158–167 (2024).
- Ancel, P. et al. Untargeted multiomics approach coupling lipidomics and metabolomics profiling reveals new insights in diabetic retinopathy. *Int. J. Mol. Sci.* **24**, (2023).

36. Mendez, K. et al. Metabolomic-derived endotypes of age-related macular degeneration (AMD): a step towards identification of disease subgroups. *Sci. Rep.* **14**, 12145 (2024).
37. Grochowski, E. T. et al. Simultaneous comparison of aqueous humor and serum metabolic profiles of diabetic and nondiabetic patients undergoing cataract surgery—a targeted and quantitative metabolomics study. *Int. J. Mol. Sci.* **24**. (2023).
38. Kataria, Y. et al. Dietary influences on tissue concentrations of phytanic acid and AMACR expression in the benign human prostate. *Prostate* **75**, 200–210 (2015).
39. Rönické, S., Kruska, N., Kahlert, S. & Reiser, G. The influence of the branched-chain fatty acids pristanic acid and Refsum disease-associated phytanic acid on mitochondrial functions and calcium regulation of hippocampal neurons, astrocytes, and oligodendrocytes. *Neurobiol. Dis.* **36**, 401–410 (2009).

Author contributions

Z.Y.W. and X.R.Z. contributed to the design of the study, analysis, and interpretation of data, and prepared all of the figures and tables. F.Y.Y. and R.R.X. performed metabolomics analysis. S.W.C., and F.Y.Y. drafted a portion of the manuscript. R.S., and T.W. took part in analyzing data and drafting a portion of the manuscript. All of the authors reviewed the manuscript.

Funding

This work was supported by the National natural science foundation of China (No. 82000733) and Beijing Municipal Science & Technology Commission (Z221100007422065). The authors would like to thank all of the participants and staff in this study.

Declarations

Consent for publication

All of the authors gave their consent to the publication. No conflict of interest exists in the submission of this manuscript, and this manuscript is approved by all of the authors for publication. The work described was original research that has not been published previously, and is not under consideration for publication elsewhere, in whole or in part.

Competing interests

The authors declare no competing interests.

Additional information

Correspondence and requests for materials should be addressed to X.-R.Z.

Reprints and permissions information is available at www.nature.com/reprints.

Publisher's note Springer Nature remains neutral with regard to jurisdictional claims in published maps and institutional affiliations.

Open Access This article is licensed under a Creative Commons Attribution-NonCommercial-NoDerivatives 4.0 International License, which permits any non-commercial use, sharing, distribution and reproduction in any medium or format, as long as you give appropriate credit to the original author(s) and the source, provide a link to the Creative Commons licence, and indicate if you modified the licensed material. You do not have permission under this licence to share adapted material derived from this article or parts of it. The images or other third party material in this article are included in the article's Creative Commons licence, unless indicated otherwise in a credit line to the material. If material is not included in the article's Creative Commons licence and your intended use is not permitted by statutory regulation or exceeds the permitted use, you will need to obtain permission directly from the copyright holder. To view a copy of this licence, visit <http://creativecommons.org/licenses/by-nc-nd/4.0/>.

© The Author(s) 2025